Research Square

Preprints are preliminary reports that have not undergone peer review.
They should not be considered conclusive, used to inform clinical practice,
or referenced by the media as validated information.

Predicted ferredoxin hydrogenase decline accompanies gut microbiome diversity loss during vonoprazan treatment: an exploratory sub-analysis of a randomized trial

Kenta Yamamoto
Nagoya University Graduate School of Medicine
Takashi Honda
honda@med.nagoya-u.ac.jp

Nagoya University Graduate School of Medicine
Kazuki Sahara
Nagoya University Graduate School of Medicine
Yosuke Inukai
Nagoya University Graduate School of Medicine
Shinya Yokoyama
Nagoya University Graduate School of Medicine
Takanori Ito
Nagoya University Graduate School of Medicine
Norihiro Imai
Nagoya University Graduate School of Medicine
Yoji Ishizu
Nagoya University Graduate School of Medicine
Yoshihiro Kadota
B Food Science Co., Ltd.
Yoshihisa Takada
Nagoya University Graduate School of Medicine
Atsushi Hashizume
Nagoya University Graduate School of Medicine
Takeshi Yamamura
Nagoya University Graduate School of Medicine
Takuya Ishikawa
Nagoya University Graduate School of Medicine
Kazuhiro Furukawa
Nagoya University Graduate School of Medicine

Hiroki Kawashima
Nagoya University Graduate School of Medicine

Research Article

Keywords: vonoprazan, 1-kestose, gut microbiome, breath hydrogen, ferredoxin hydrogenase, PICRUSt2, microbial diversity

Posted Date: November 19th, 2026

DOI: https://doi.org/10.21203/rs.3.rs-10992142/v1

License: This work is licensed under a Creative Commons Attribution 4.0 International License.
Read Full License

Additional Declarations: Competing interest reported. Yoshihiro Kadota is an employee of B Food Science Co., Ltd., which manufactured the 1-kestose used in the randomized trial. The remaining authors declare no competing interests.

Abstract

Background

Strong gastric acid suppression alters the gut microbiota, but the functional meaning of the resulting loss of bacterial diversity remains unclear.

Methods

We performed an exploratory sub-analysis of a randomized, double-blind, placebo-controlled pilot trial of 1-kestose during eight weeks of vonoprazan treatment. The analysis included 24 participants with matched baseline fasting breath-gas measurements, baseline and week-8 16S rRNA profiles, PICRUSt2-predicted Enzyme Commission abundances, and fecal short-chain fatty acids. Three consecutive baseline breath measurements were summarized by their participant-level median. Predicted Ferredoxin hydrogenase abundance was normalized per million predicted EC counts.

Results

Baseline breath H_2 measurements were repeatable (ICC [2, 1] = 0.857), and higher predicted Ferredoxin hydrogenase abundance was associated with higher median breath H_2 after adjustment for simultaneously measured median breath CO (β = 3.979 ppb per RPM; 95% CI, 0.253–7.704; P = 0.037). Predicted Ferredoxin hydrogenase abundance decreased in the placebo group (median change, − 92.6 RPM; q = 0.006) but did not show a statistically significant within-group decrease in the 1-kestose group (median change, − 20.0 RPM; q = 0.500). Changes in predicted Ferredoxin hydrogenase abundance correlated positively with changes in Simpson diversity (Spearman ρ = 0.420; P = 0.041), while cross-sectional values at either time point were not associated. Fecal short-chain fatty acids did not provide independent positive validation of the hydrogenase signal.

Conclusions

These findings suggest that vonoprazan-associated diversity loss was accompanied by a decline in predicted ferredoxin-linked hydrogen-metabolism potential and that 1-kestose may attenuate this functional change.

Trial registration

University Hospital Medical Information Network Clinical Trials Registry (UMINCTR), UMIN000028803 registered 24 August 2017. Japan Registry of Clinical Trials (jRCT), jRCTs041190016 registered 10 April 2019.

1. Introduction

Proton pump inhibitors (PPIs) and potassium-competitive acid blockers (PCABs) weaken the gastric acid barrier and can alter the intestinal microbial community. Human cohort and interventional studies have reported enrichment of oral-associated organisms, depletion of selected commensal taxa, and changes in overall community structure during acid suppression [1–5]. In our preceding randomized pilot trial, eight weeks of vonoprazan treatment was accompanied by a significant reduction in Simpson diversity in the placebo group, whereas no significant reduction was observed among participants receiving the prebiotic 1-kestose [6]. That result established a broad ecological signal, but a diversity index alone does not identify which microbial function may have been preferentially lost.

The gut microbiome comprises a diverse yet functionally interconnected anaerobic ecosystem [7]. Molecular hydrogen (H_2) is a major end product of microbial carbohydrate fermentation, and its concentration reflects the balance between H_2 production, microbial consumption through methanogenesis, acetogenesis, sulfate reduction and respiration, intestinal handling, and excretion [8–11]. Hydrogen metabolism is therefore not confined to a single bacterial genus: hydrogenase genes are widely distributed across gut bacteria and span multiple enzyme classes and physiological roles [11–14]. This functional breadth makes hydrogen metabolism a plausible lens through which an apparently nonspecific reduction in community diversity may be interpreted.

Ferredoxin-linked hydrogenases are particularly relevant to anaerobic fermentation because they connect ferredoxin redox metabolism with H_2 turnover; in fermentative contexts, some enzymes use reduced ferredoxin to support H_2 evolution and electron disposal [12–14]. Recent metagenomic, transcriptomic, culture, and biochemical evidence indicates that ferredoxin-linked [FeFe]-hydrogenases are abundant and active among major gut fermenters [14]. Other ferredoxin-linked hydrogenase systems can use ferredoxin and NADH simultaneously, underscoring that distinct hydrogenase classes should not be conflated [15]. Breath H_2 provides a noninvasive host-level readout of intestinal microbial gas production, although it is shaped by production, consumption, transit, diffusion, and pulmonary excretion and is not a direct enzyme assay [16–18]. Pairing fasting breath H_2 with a 16S-based prediction of Ferredoxin hydrogenase abundance could therefore test whether the inferred functional signal has a measurable external correlate.

We conducted an exploratory sub-analysis of participants from the preceding 1-kestose trial who had complete breath-gas, microbiome, predicted functional, and fecal short-chain fatty acid data. We first examined whether baseline predicted Ferredoxin hydrogenase abundance was associated with fasting breath H_2 after adjustment for simultaneously measured breath CO. We then assessed longitudinal changes in a predefined panel of hydrogenase-related ECs, determined whether change in predicted Ferredoxin hydrogenase abundance tracked change in Simpson diversity, and evaluated fecal short-chain fatty acids as a complementary metabolic measure. PICRUSt2 was used to infer functional potential from the 16S profiles [19]. The aim was not to establish enzymatic activity from 16S data, but to clarify

whether vonoprazan-associated diversity loss was accompanied by a coherent predicted hydrogen-metabolism signal and whether that signal differed during 1-kestose administration.

2. Results

2.1 Study population and baseline characteristics

Forty participants were randomized in this trial, of whom 32 were included in the per-protocol microbiome analysis. The present complete-case sub-analysis included 24 participants (75% of the per-protocol cohort): 12 assigned to placebo and 12 assigned to 1-kestose (Supplementary Figure S1). All 24 had three baseline breath-gas measurements, matched baseline and week-8 microbiome profiles, PICRUSt2-predicted EC abundances, Simpson diversity indices, and fecal SCFA measurements.

The median age was 72.5 years (IQR, 64.8–77.0), and 19 participants (79.2%) were men. Baseline body mass index, lesion size, alcohol use, smoking history, Simpson diversity, and predicted Ferredoxin hydrogenase abundance were broadly similar in descriptive terms between randomized groups (Table 1). Men accounted for 8 of 12 participants in the placebo group and 11 of 12 in the 1-kestose group. Detectable methane, defined descriptively as a participant-level median greater than 0 ppb, was present in 9 placebo participants and 3 1-kestose participants. Because this was a small selected subset of the randomized trial, no hypothesis tests were performed for baseline characteristics.

Table 1
Baseline characteristics of the sub-analysis cohort

Characteristic	Overall (n = 24)	Placebo (n = 12)	1-kestose (n = 12)
Clinical characteristics			
Age, years	72.5 (64.8–77.0)	74.5 (67.2–77.5)	70.0 (62.8–73.2)
Male sex, n (%)	19 (79.2%)	8 (66.7%)	11 (91.7%)
Body mass index, kg/m²	22.7 (20.7–24.5)	22.7 (20.5–24.0)	22.7 (20.8–24.5)
Helicobacter pylori status, n (%)			
Negative	5 (20.8%)	3 (25.0%)	2 (16.7%)
After eradication	15 (62.5%)	8 (66.7%)	7 (58.3%)
Positive	4 (16.7%)	1 (8.3%)	3 (25.0%)
Gastric cancer, n (%)	21 (87.5%)	10 (83.3%)	11 (91.7%)
Lesion size, mm	14.0 (10.8–17.2)	12.5 (11.2–18.5)	14.5 (10.8–16.2)
Alcohol use, n (%)	12 (50.0%)	5 (41.7%)	7 (58.3%)
Smoking history, n (%)	15 (62.5%)	8 (66.7%)	7 (58.3%)
Pack-years	15.6 (0.0–40.0)	20.0 (0.0–45.0)	5.1 (0.0–26.9)
Supplement use, n (%)	7 (29.2%)	3 (25.0%)	4 (33.3%)
Bristol stool scale, n (%)			
Type 2	5 (20.8%)	4 (33.3%)	1 (8.3%)
Type 3	7 (29.2%)	2 (16.7%)	5 (41.7%)
Type 4	8 (33.3%)	3 (25.0%)	5 (41.7%)
Type 5	1 (4.2%)	1 (8.3%)	0 (0.0%)
Type 6	3 (12.5%)	2 (16.7%)	1 (8.3%)
Baseline analytical measures			
Breath H_2, ppb	1789.3 (1107.8–2457.8)	2032.2 (1022.0–2690.1)	1550.3 (1179.4–1880.5)
Breath CO, ppb	1991.4 (1502.3–2490.1)	2342.8 (1594.7–2616.2)	1865.5 (1502.3–2427.4)

Values are median (IQR) or n (%). Breath gases are medians of three baseline measurements. Detectable CH_4 denotes median > 0 ppb. Ferredoxin hydrogenase = predicted EC abundance / sum of 1,815 ECs × 10^6. Baseline P values were not calculated.

Characteristic	Overall (n = 24)	Placebo (n = 12)	1-kestose (n = 12)
Clinical characteristics			
Breath CH_4, ppb	185.8 (0.0–1618.0)	564.0 (278.7–2463.1)	0.0 (0.0–204.8)
Detectable breath CH_4, n (%)	12 (50.0%)	9 (75.0%)	3 (25.0%)
Simpson diversity index	0.889 (0.848–0.907)	0.892 (0.871–0.904)	0.864 (0.802–0.907)
Ferredoxin hydrogenase, RPM	214.0 (159.5–259.3)	222.8 (204.5–285.3)	178.0 (99.3–242.2)

Values are median (IQR) or n (%). Breath gases are medians of three baseline measurements. Detectable CH_4 denotes median > 0 ppb. Ferredoxin hydrogenase = predicted EC abundance / sum of 1,815 ECs × 10^6. Baseline P values were not calculated.

2.2 Baseline breath H_2 repeatability and association with predicted Ferredoxin hydrogenase

The three baseline breath H_2 measurements showed high repeatability (ICC [2, 1] = 0.857; participant-level bootstrap 95% CI, 0.629–0.986), and the median within-participant CV was 4.5% (IQR, 2.4–8.5%) (Fig. 1A). The participant-level median breath H_2 concentration was 1,789.3 ppb (IQR, 1,107.8–2,457.8 ppb).

In the prespecified OLS model including simultaneously measured median breath CO as a covariate, higher baseline predicted Ferredoxin hydrogenase abundance was positively associated with median breath H_2 concentration (unstandardized β = 3.979 ppb per RPM; SE = 1.791; 95% CI, 0.253–7.704; P = 0.037; standardized β = 0.233) (Fig. 1B). A participant-level bootstrap yielded a 95% CI of 0.271–8.023 ppb per RPM, and a Freedman–Lane permutation test conditional on CO gave P = 0.039. The coefficient remained positive in all leave-one-out analyses (range, 3.053–5.323 ppb per RPM), although the corresponding P values ranged from 0.009 to 0.122. Sensitivity estimates were consistently positive, but evidence was attenuated with HC3 robust variance estimation (95% CI, − 0.480 to 8.438; P = 0.078) and after log transformation (Supplementary Figure S2). The result therefore supports an exploratory positive association, with uncertainty reflecting the small sample.

2.3 Longitudinal changes in predicted Ferredoxin hydrogenase abundance

Predicted Ferredoxin hydrogenase abundance decreased from a median of 222.8 RPM (IQR, 204.5–285.3) at baseline to 146.9 RPM (IQR, 113.9–184.5) at week 8 in the placebo group (median change, − 92.6 RPM; exact Wilcoxon P = 0.001; BH q = 0.006) (Fig. 2A). In the 1-kestose group, the corresponding medians were 178.0 RPM (IQR, 99.3–242.2) and 123.4 RPM (IQR, 87.2–191.3), and the within-group change was not statistically significant (median change, − 20.0 RPM; exact Wilcoxon P = 0.233; q = 0.500) (Fig. 2B).

In the direct change-score comparison, the mean decline was 68.7 RPM smaller in the 1-kestose group than in the placebo group (95% CI, 7.6–129.9 RPM; P = 0.029; HC3-robust P = 0.036) (Fig. 2C). The contrast was supported by label permutation testing (P = 0.030), a stratified bootstrap 95% CI of 12.9–123.7 RPM, and log-transformed change-score analysis (P = 0.030). However, baseline-adjusted ANCOVA produced a smaller, non-significant adjusted week-8 difference of 29.3 RPM (95% CI, − 19.3 to 77.9 RPM; P = 0.224; HC3-robust P = 0.301) (Supplementary Table S2). Thus, the decline was more evident in the placebo group and the data were compatible with an attenuated decline during 1-kestose administration.

Across the complete predefined panel of six hydrogenase-related ECs, only the within-placebo change in Ferredoxin hydrogenase remained significant after correction for multiple comparisons. No between-group change-score comparison met an FDR threshold of $q < 0.05$ (Ferredoxin hydrogenase, q = 0.088) (Supplementary Figure S3 and Supplementary Table S1). Coenzyme F420 hydrogenase showed a nominal between-group difference (P = 0.018; q = 0.088), but it was detected in only 13 of 48 longitudinal samples and was treated as descriptive. The other hydrogenase-related ECs, including Hydrogenase (acceptor), showed no significant between-group change.

2.4 Predicted Ferredoxin hydrogenase change tracked Simpson diversity change

Predicted Ferredoxin hydrogenase abundance was not significantly associated with Simpson diversity in cross-sectional analyses at baseline (Spearman ρ = 0.204; P = 0.338) or week 8 (ρ = 0.093; P = 0.665). In contrast, their eight-week changes were positively correlated (Spearman ρ = 0.420; P = 0.041; permutation P = 0.040; Pearson r = 0.411; P = 0.046; Kendall τ-b = 0.275; P = 0.059) (Fig. 3). After adjustment for randomized group, the partial Spearman correlation was ρ = 0.476 (P = 0.022) (Supplementary Figure S4A).

In the group-adjusted linear model, a 100-RPM greater change in predicted Ferredoxin hydrogenase abundance was associated with a 0.038 greater change in Simpson diversity (95% CI, − 0.0001 to 0.0767; P = 0.051; HC3-robust 95% CI, 0.0035–0.0731; P = 0.032). The association remained positive in a log-change model (P = 0.007; HC3-robust P = 0.013) but was attenuated after additional adjustment for baseline Simpson diversity (P = 0.088) (Supplementary Table S4). Group-specific rank correlations were directionally consistent in the placebo (ρ = 0.573; P = 0.051) and 1-kestose groups (ρ = 0.441; P = 0.152), with no evidence of a group interaction (P = 0.748).

All 24 leave-one-out estimates remained positive (ρ range, 0.344–0.494), although only 14 of the 24 corresponding P values were below 0.05. The participant-level bootstrap 95% CI for the overall Spearman correlation included zero (− 0.041 to 0.728) (Supplementary Figure S4B and Supplementary Table S3). Because both variables were derived from the same 16S dataset, this directionally consistent but statistically borderline finding indicates internal concordance during microbiome restructuring rather than independent functional validation or causation.

2.5 Fecal short-chain fatty acids did not independently support the hydrogenase signal

Fecal SCFA concentrations were available at both time points for all 24 participants. None of the six measured SCFAs or two derived indicators showed a significant within-group change after BH correction in either group, and no between-group comparison of eight-week change was significant (all $q \geq 0.351$) (Supplementary Table S5 and Supplementary Figure S5A). The largest numerical separation was observed for acetate, for which the Hodges–Lehmann shift in change for 1-kestose minus placebo was − 15.36 μmol/g (permutation $P = 0.052$; $q = 0.351$).

At baseline, none of the eight fecal SCFA indicators was associated with predicted Ferredoxin hydrogenase abundance (all $q = 0.961$), CO-adjusted breath H_2 (all $q \geq 0.135$), or Simpson diversity (all $q \geq 0.843$). Changes in fecal SCFAs were also not associated with changes in Simpson diversity (all $q \geq 0.904$) (Supplementary Table S6 and Supplementary Figure S5B).

Unadjusted change-score analyses showed inverse associations between changes in several SCFAs and predicted Ferredoxin hydrogenase abundance. These associations were sensitive to regression-to-the-mean and baseline adjustment: after adjustment for randomized group and the ranked baseline values of both the corresponding SCFA and Ferredoxin hydrogenase, all estimates were attenuated and none remained significant (partial ρ, − 0.397 to 0.134; all $q \geq 0.467$) (Supplementary Tables S6 and S7). Fecal SCFA concentrations therefore did not provide independent positive validation of the predicted Ferredoxin hydrogenase signal.

3. Discussion

This sub-analysis gives a functional interpretation to the diversity change observed in the preceding trial. During eight weeks of vonoprazan treatment, predicted Ferredoxin hydrogenase abundance declined markedly in the placebo group, and the degree of its decline tracked the reduction in Simpson diversity across participants. The association was specific to change over time rather than to cross-sectional differences: participants with more Ferredoxin hydrogenase at baseline did not simply have more diverse microbiota. These findings support the view that the previously reported diversity loss was accompanied by contraction of a predicted ferredoxin-linked hydrogen-metabolism component of the community.

The breath-gas analysis strengthens that interpretation. Three fasting breath H_2 measurements were reproducible, and the participant-level median was positively associated with predicted Ferredoxin hydrogenase abundance after adjustment for simultaneously measured CO. The longitudinal change-score contrast was also compatible with a smaller Ferredoxin hydrogenase decline during 1-kestose administration. Taken together, the clearest message is not that 1-kestose definitively preserved H_2 production or reaction direction, but that the vonoprazan-associated ecological change had a coherent ferredoxin-linked hydrogen-metabolism signature and that this signature was less pronounced under 1-kestose in the principal change-score analysis.

Hydrogen metabolism is a biologically plausible bridge between microbial community structure and an external breath phenotype. Colonic H_2 arises mainly from anaerobic fermentation and is subsequently partitioned among exhalation and microbial consumption pathways [8–11]. Hydrogenases are distributed across many gut taxa, and ferredoxin-linked [FeFe]-hydrogenases support electron disposal and fermentative growth in diverse Bacteroidetes and Firmicutes [11–15]. Thus, the present EC signal should not be read as a surrogate for one named bacterium or a single reaction direction. It more likely summarizes distributed ferredoxin-linked hydrogen-metabolism potential. At the same time, breath H_2 is influenced by substrate availability, intestinal transit, competing H_2 consumers, diffusion, and pulmonary elimination [16–18]. The observed association is therefore valuable as external concordance, but it does not establish a one-to-one relationship between a predicted enzyme count and in-vivo H_2 flux.

The 1-kestose finding is consistent with a prebiotic effect on community organization rather than a direct pharmacological action on a single enzyme. Prebiotics are substrates selectively utilized by host microorganisms, and 1-kestose is the smallest component of fructooligosaccharides with documented bifidogenic and fermentative effects [20, 21]. In experimental animals, 1-kestose alters the cecal microbiota and increases fermentation products, including butyrate [22]. In this trial, 1-kestose was associated with preservation of Simpson diversity and attenuation of the vonoprazan-associated increase in Streptococcus [6]. Here, however, fecal SCFA concentrations neither changed between groups nor positively validated the hydrogenase signal. This is not necessarily contradictory because fecal SCFA concentrations reflect the net balance among microbial production and utilization, host absorption, and intestinal transit rather than production flux alone [23, 24].

The results also fit the wider literature on acid-suppression-associated dysbiosis. PPIs and PCABs can promote oral-to-gut microbial transmission and alter taxa involved in colonization resistance and fermentation [1–5, 25]. Epidemiological studies have linked acid suppression to Clostridioides difficile infection, and meta-analyses report a moderate association with small intestinal bacterial overgrowth [26–28]. These clinical associations are not evidence that loss of Ferredoxin hydrogenase causes those outcomes, and our study did not measure infection, overgrowth, or gastrointestinal symptoms. Nevertheless, identifying a functional change that accompanies diversity loss may help move the discussion beyond a nonspecific label of dysbiosis. A hydrogen-metabolism axis is particularly relevant because it integrates fermentation, redox balance, microbial cross-feeding, and an accessible breath signal.

Several limitations should be considered. This was an exploratory complete-case sub-analysis of 24 participants from this trial, with 12 per group, no sample-size calculation, and multiple related analyses. The direct change-score and ANCOVA treatment contrasts were not concordant, and several sensitivity estimates crossed the null. Breath gas was measured only at baseline, without a carbohydrate load, so longitudinal coupling between breath H_2 and the predicted EC could not be tested. PICRUSt2 infers genomic potential from 16S profiles and does not measure gene abundance by shotgun metagenomics, transcription, protein abundance, or catalytic activity [19]. The EC label “Ferredoxin hydrogenase” does not resolve hydrogenase subgroup, directionality, organismal source, or actual H_2 flux. Simpson diversity

and the predicted EC were derived from the same 16S dataset, making their change correlation an internal consistency result rather than independent validation. Finally, the complete-case subset and baseline methane imbalance may limit generalizability. These constraints favor interpretation based on effect direction and consistency rather than a single P value.

3.1 Conclusions

In participants receiving vonoprazan, loss of gut microbial diversity was accompanied by a decline in predicted Ferredoxin hydrogenase abundance, and the predicted function showed an independent positive association with baseline fasting breath H_2. The decline was most evident in the placebo group and was attenuated in the principal 1-kestose change-score comparison. These exploratory findings identify hydrogen metabolism as a plausible functional dimension of acid-suppression-associated microbiome change and provide a focused hypothesis for validation using longitudinal breath measurements, shotgun metagenomics, and direct functional assays.

4. Methods

4.1 Study design and participants

This study was an exploratory sub-analysis of a previously reported prospective, randomized, double-blind, placebo-controlled pilot trial conducted at Nagoya University Hospital [6]. Of 40 randomized participants, 32 were included in the per-protocol microbiome analysis, and the present analysis included 24 participants (12 per group) with complete baseline breath-gas measurements, paired baseline and week-8 microbiome data, PICRUSt2-predicted EC abundances, Simpson diversity, and fecal SCFA measurements. No additional sample-size calculation was performed, and all analyses were considered exploratory. This report was prepared in accordance with the CONSORT 2025 reporting guidelines, as applicable to an sub-analysis of a randomized trial. Full details of the trial design and conduct are reported elsewhere [6].

This trial was approved by the Nagoya University Bioethics Committee (approval no. 2015 – 0420 6928), conducted in accordance with the Declaration of Helsinki, and registered in the University Hospital Medical Information Network Clinical Trials Registry (UMIN-CTR; UMIN000028803; 24 August 2017) and the Japan Registry of Clinical Trials (jRCT; jRCTs041190016; 10 April 2019). Written informed consent was obtained from all participants [6].

4.2 Randomization, intervention, and specimen collection

Participants were randomized 1:1 through a web-based system at Nagoya University Hospital, with age, sex, and Helicobacter pylori status used as stratification factors. Participants and study personnel were masked to allocation. The 1-kestose group received 1-kestose of greater than 98% purity at 10 g/day, and the placebo group received maltose of greater than 92% purity at 5 g/day. All participants started

vonoprazan 20 mg/day on the second day after endoscopic treatment and continued the assigned study product with vonoprazan for eight weeks [6].

Stool samples were collected before treatment and at week 8. Baseline samples were collected during hospitalization, and week-8 samples were collected by participants at home. Samples were promptly frozen and stored at − 80°C until analysis. Microbiome sample identifiers were linked one-to-one to the clinical baseline and week-8 identifiers before analysis.

4.3 Breath-gas measurement and preprocessing

Breath gas was measured only at baseline. Samples were obtained in the early morning after an overnight fast, without administration of glucose, lactulose, or another test substrate. Three consecutive samples were collected on the same day. Hydrogen, CO, and methane concentrations were measured in ppb with a sensor gas chromatograph (SGHA, Nissha FIS Inc., Japan) and processed using SGC Analysis Software, as described for the same measurement platform [18]. The participant-level median of the three measurements was used for each gas. Methane detectability was defined descriptively as a median concentration greater than 0 ppb.

No instrument-specific equation was available to transform H_2 into a calibrated CO-corrected concentration. Accordingly, the primary analysis adjusted statistically for the simultaneously measured median CO concentration. The prespecified model was median $H_{2i} = \beta_0 + \beta_1$(Ferredoxin hydrogenase RPM_i) + β_2(median CO_i) + ε_i. Thus, 'CO-adjusted breath H_2' denotes the conditional H_2 association estimated from this model and not a separately transformed concentration. The collection conditions followed the general principles used for fasting breath sampling and breath-test methodology [16–18].

4.4 16S rRNA gene sequencing and diversity

Fecal bacterial DNA extraction and 16S rRNA gene sequencing followed the parent protocol [6]. Briefly, the V3–V4 region was amplified and sequenced on an Illumina MiSeq using MiSeq Reagent Kit v3 (600 cycles; paired-end reads, 2 × 284 bp). Sequence processing was performed in QIIME 2 version 2019.10, and denoising used DADA2 with default settings [29, 30]. Taxonomic assignment used the SILVA 138 database [31, 32]. Simpson diversity values from the parent microbiome analysis were used. Change was calculated as week 8 minus baseline. The raw amplicon sequencing data have been deposited in the DDBJ Sequence Read Archive and are publicly available under BioProject accession number PRJDB45839.

4.5 PICRUSt2 functional prediction and hydrogenase-related EC panel

PICRUSt2 version 2021.11 was used to infer microbial functional potential from the 16S profiles [19]. The available output contained predicted abundances for 1,815 EC features. Because total predicted EC abundance varied between samples, each EC was normalized within sample by dividing its predicted abundance by the sum of all 1,815 EC abundances and multiplying by 10^6. These normalized values are

reported as RPM. They represent predicted functional potential and not direct measurements of genes, transcripts, proteins, enzyme activity, or metabolic flux.

Ferredoxin hydrogenase (EC 1.12.7.2), annotated as hydrogen:ferredoxin oxidoreductase, was selected as the principal hydrogenase-related feature because it links ferredoxin redox metabolism with H_2 turnover in anaerobic organisms [12–14]. To avoid selective reporting, all six hydrogenase-related ECs present in the PICRUSt2 table were analyzed as a predefined panel: Hydrogen dehydrogenase (NADP+) (EC 1.12.1.3), Cytochrome-c3 hydrogenase (EC 1.12.2.1), Ferredoxin hydrogenase (EC 1.12.7.2), Coenzyme F420 hydrogenase (EC 1.12.98.1), 5,10-methenyltetrahydromethanopterin hydrogenase (EC 1.12.98.2), and Hydrogenase (acceptor) (EC 1.12.99.6). Features detected in fewer than 50% of the 48 longitudinal samples were classified as sparse and interpreted descriptively. EC change was calculated as week 8 minus baseline; log sensitivity analyses used ln (RPM + 1).

4.6 Fecal short-chain fatty acids

Fecal acetate, propionate, butyrate, isobutyrate, valerate, and isovalerate were measured at baseline and week 8 by gas chromatography–mass spectrometry using a GCMS-QP2010 Ultra system (Shimadzu, Kyoto, Japan) fitted with an Rtx-1701 column (Restek, Bellefonte, PA, USA), following the parent protocol [6, 22]. Concentrations were expressed as μmol/g feces. Total SCFA was the sum of the six measured acids, and BCFA was the sum of isobutyrate and isovalerate. Change was calculated as week 8 minus baseline.

4.7 Analysis framework and outcomes

The principal cross-sectional analysis examined the association between baseline median breath H_2 and baseline predicted Ferredoxin hydrogenase RPM after adjustment for median breath CO. The principal longitudinal analysis evaluated group-specific and between-group changes in predicted Ferredoxin hydrogenase abundance. Supporting analyses evaluated the complete six-EC panel, the association between changes in predicted Ferredoxin hydrogenase and Simpson diversity, and fecal SCFAs as complementary metabolic measures. Because these analyses were hypothesis-generating, and based on a small complete-case subset, effect estimates, confidence intervals, consistency across sensitivity analyses, and multiplicity-adjusted results were emphasized.

4.8 Statistical analysis

Continuous variables are summarized as median (IQR), and categorical variables as number (percentage). Baseline characteristics were presented descriptively without P values. Repeatability of the three breath H_2 measurements was quantified using the two-way-random, absolute-agreement, single-measure ICC (2,1), with a 20,000-resample participant-level bootstrap confidence interval; interpretation followed published ICC guidance [33]. Within-participant variability was also summarized by the CV.

The baseline H_2–Ferredoxin association was estimated by OLS with median breath CO as a covariate. Inference for the Ferredoxin coefficient used a two-sided t test and conventional model-based 95% CI. Supporting analyses used 20,000 participant-level bootstrap resamples, a 20,000-iteration Freedman–

Lane permutation test conditional on CO, HC3 heteroskedasticity-consistent standard errors, log transformations, additional smoking or pack-year adjustment, and leave-one-out refitting [34, 35]. Residual-versus-fitted, normal quantile–quantile, and Cook-distance diagnostics were examined.

Within-group EC changes were assessed with exact two-sided signed-rank randomization tests. Between-group differences in change scores were estimated by OLS as 1-kestose minus placebo, with conventional and HC3 inference, 20,000 group-label permutations, stratified bootstrap confidence intervals, and log-change sensitivity analyses. A baseline-adjusted ANCOVA modeled week-8 RPM as the outcome with baseline RPM and group as predictors. BH correction controlled the FDR across the six ECs separately within each inferential family [36].

The association between Ferredoxin hydrogenase change and Simpson change was assessed primarily by Spearman rank correlation, with participant-level bootstrap confidence intervals and permutation P values. Pearson correlation and Kendall τ-b were complementary. A group-adjusted partial Spearman correlation was obtained by correlating residuals from the ranks of each change score after regression on randomized group. Group-adjusted linear models reported Simpson change per 100-RPM Ferredoxin change, with conventional and HC3 inference. Log-change, baseline-Simpson adjustment, group interaction, group-specific correlation, and leave-one-out analyses assessed sensitivity.

Within-group SCFA changes were tested using exact two-sided signed-rank randomization tests. Between-group change differences used a 20,000-label-permutation rank-sum test with Hodges–Lehmann shifts. Associations were estimated using Spearman or partial Spearman correlations. Because change scores were associated with baseline values, the main SCFA–Ferredoxin sensitivity analysis adjusted for randomized group and the ranked baseline values of both variables. BH correction was performed across the eight SCFA indicators separately within each inferential family. All tests were two-sided; nominal $P < 0.05$ and BH-adjusted $q < 0.05$ were used as descriptive thresholds. Analyses and figures were reproduced in Python 3.12 using the archived Jupyter notebooks and analysis scripts supplied with this study.

Abbreviations

ANCOVA
analysis of covariance
BCFA
branched-chain fatty acids
BH
Benjamini–Hochberg
CH_4
methane
CI
confidence interval

CO
carbon monoxide
CV
coefficient of variation
EC
Enzyme Commission
FDR
false discovery rate
H_2
hydrogen
ICC
intraclass correlation coefficient
IQR
interquartile range
OLS
ordinary least squares
PCAB
potassium-competitive acid blocker
PPI
proton pump inhibitor
RPM
normalized predicted abundance per million
SCFA
short-chain fatty acid.

Declarations

Acknowledgments

We thank Ms. Akina Ooishi of the Department of Gastroenterology and Hepatology, Nagoya University Graduate School of Medicine, for technical assistance with DNA isolation and 16S rRNA gene sequencing. We also acknowledge the Division for Medical Research Engineering, Nagoya University Graduate School of Medicine, for use of the MiSeq platform.

Funding

The parent trial was partially funded by B Food Science Co., Ltd. The funder was not involved in the study design or manuscript writing [6].

Competing interests

Yoshihiro Kadota is an employee of B Food Science Co., Ltd., which manufactured the 1-kestose used in the randomized trial [6]. The remaining authors declare no competing interests.

Data Availability Statement

The raw 16S rRNA gene amplicon sequencing data have been deposited in the DDBJ Sequence Read Archive (DRA) and are publicly available under BioProject accession number PRJDB45839 (Run accession numbers DRR1207604–DRR1207671). Processed microbiome and short-chain-fatty-acid data from the parent trial are publicly available in the Nagoya University Academic Institutional Repository (http://hdl.handle.net/2237/0002004261). Additional de-identified participant-level clinical data used in this secondary analysis are not publicly available because the informed consent and study protocol did not include provisions for sharing participant-level data with third parties. The reproducible Jupyter notebooks underlying this secondary analysis are available from the corresponding author upon reasonable request.

Ethics approval

This trial was approved by the Nagoya University Bioethics Committee (approval no. 2015-0420 6928), conducted in accordance with the Declaration of Helsinki, and registered in the University Hospital Medical Information Network Clinical Trials Registry (UMIN-CTR; UMIN000028803; 24 August 2017) and the Japan Registry of Clinical Trials (jRCT; jRCTs041190016; 10 April 2019).

Informed consent

Written informed consent was obtained from all participants in the trial.

Consent for publication

Not applicable.

Author contributions

Kenta Yamamoto conceived and designed the secondary analysis. Kenta Yamamoto curated the analytical dataset and performed the statistical, microbiome, and PICRUSt2 functional analyses. Takashi Honda, Takanori Ito, Yoji Ishizu, Yoshihisa Takada, Atsushi Hashizume and Kenta Yamamoto interpreted the results and drafted the manuscript. Norihiro Imai, Yoshihiro Kadota, Takeshi Yamamura, Takuya Ishikawa, Kazuhiro Furukawa, and Hiroki Kawashima supervised the work. All authors contributed to the clinical and scientific interpretation of the findings, critically revised the manuscript for important intellectual content, approved the final version, and agreed to be accountable for the work.

AI use disclosure

Generative artificial intelligence tools were used to assist with language editing, readability improvement, literature organization, and checking or refining Python scripts for statistical analysis. The tools were not

used to determine the study hypothesis, generate data, or make final scientific interpretations or conclusions. All analyses, citations, interpretations, and manuscript content were reviewed and verified by the authors, who take full responsibility for the integrity and accuracy of the work.

References

1. Imhann F, et al. Proton pump inhibitors affect the gut microbiome. Gut. 2016;65:740–8. https://doi.org/10.1136/gutjnl-2015-310376.
2. Jackson MA, et al. Proton pump inhibitors alter the composition of the gut microbiota. Gut. 2016;65:749–56. https://doi.org/10.1136/gutjnl-2015-310861.
3. Freedberg DE, et al. Proton pump inhibitors alter specific taxa in the human gastrointestinal microbiome: a crossover trial. Gastroenterology. 2015;149:883–5. https://doi.org/10.1053/j.gastro.2015.06.043. .e9.
4. Zhu J, et al. Compared to histamine-2 receptor antagonist, proton pump inhibitor induces stronger oral-to-gut microbial transmission and gut microbiome alterations: a randomised controlled trial. Gut. 2024;73:1087–97. https://doi.org/10.1136/gutjnl-2023-330168.
5. Otsuka T, et al. Influence of potassium-competitive acid blocker on the gut microbiome of *Helicobacter pylori*-negative healthy individuals. Gut. 2017;66:1723–5. https://doi.org/10.1136/gutjnl-2016-313312.
6. Furune S, et al. Effects of 1-kestose on microbiome changes caused by vonoprazan: a randomized, double-blind, placebo-controlled pilot study. J Gastroenterol Hepatol. 2024;39:480–8. https://doi.org/10.1111/jgh.16445.
7. Human Microbiome Project Consortium. Structure, function and diversity of the healthy human microbiome. Nature. 2012;486:207–14. https://doi.org/10.1038/nature11234.
8. Levitt MD. Production and excretion of hydrogen gas in man. N Engl J Med. 1969;281:122–7. https://doi.org/10.1056/NEJM196907172810303.
9. Christl SU, Murgatroyd PR, Gibson GR, Cummings JH. Production, metabolism, and excretion of hydrogen in the large intestine. Gastroenterology. 1992;102:1269–77. https://doi.org/10.1016/0016-5085(92)90765-Q.
10. Gibson GR, Cummings JH, Macfarlane GT. Alternative pathways for hydrogen disposal during fermentation in the human colon. Gut. 1990;31:679–83. https://doi.org/10.1136/gut.31.6.679.
11. Wolf PG, Biswas A, Morales SE, Greening C, Gaskins H. R. H_2 metabolism is widespread and diverse among human colonic microbes. Gut Microbes. 2016;7:235–45. https://doi.org/10.1080/19490976.2016.1182288.
12. Greening C, et al. Genomic and metagenomic surveys of hydrogenase distribution indicate H_2 is a widely utilised energy source for microbial growth and survival. ISME J. 2016;10:761–77. https://doi.org/10.1038/ismej.2015.153.

13. Vignais PM, Billoud B, Meyer J. Classification and phylogeny of hydrogenases. FEMS Microbiol Rev. 2001;25:455–501. https://doi.org/10.1111/j.1574-6976.2001.tb00587.x.
14. Welsh C, et al. A widespread hydrogenase supports fermentative growth of gut bacteria in healthy people. Nat Microbiol. 2025;10:2686–701. https://doi.org/10.1038/s41564-025-02154-w.
15. Schut GJ, Adams MWW. The iron-hydrogenase of *Thermotoga maritima* utilizes ferredoxin and NADH synergistically: a new perspective on anaerobic hydrogen production. J Bacteriol. 2009;191:4451–7. https://doi.org/10.1128/JB.01582-08.
16. Gasbarrini A et al. Methodology and indications of H_2-breath testing in gastrointestinal diseases: the Rome Consensus Conference. Aliment. Pharmacol. Ther. 29 Suppl. 1, 1–49 (2009). https://doi.org/10.1111/j.1365-2036.2009.03951.x
17. Rezaie A, et al. Hydrogen and methane-based breath testing in gastrointestinal disorders: the North American Consensus. Am J Gastroenterol. 2017;112:775–84. https://doi.org/10.1038/ajg.2017.46.
18. Uetsuki K, et al. Measurement of fasting breath hydrogen concentration as a simple diagnostic method for pancreatic exocrine insufficiency. BMC Gastroenterol. 2021;21:211. https://doi.org/10.1186/s12876-021-01776-8.
19. Douglas GM, et al. PICRUSt2 for prediction of metagenome functions. Nat Biotechnol. 2020;38:685–8. https://doi.org/10.1038/s41587-020-0548-6.
20. Gibson GR, et al. Expert consensus document: the International Scientific Association for Probiotics and Prebiotics consensus statement on the definition and scope of prebiotics. Nat Rev Gastroenterol Hepatol. 2017;14:491–502. https://doi.org/10.1038/nrgastro.2017.75.
21. Tochio T, Kadota Y, Tanaka T, Koga Y. 1-Kestose, the smallest fructooligosaccharide component, which efficiently stimulates *Faecalibacterium prausnitzii* as well as bifidobacteria in humans. Foods. 2018;7:140. https://doi.org/10.3390/foods7090140.
22. Tochio T, et al. An alteration in the cecal microbiota composition by feeding of 1-kestose results in a marked increase in the cecal butyrate content in rats. PLoS ONE. 2016;11:e0166850. https://doi.org/10.1371/journal.pone.0166850.
23. Boets E, et al. Systemic availability and metabolism of colonic-derived short-chain fatty acids in healthy subjects: a stable isotope study. J Physiol. 2017;595:541–55. https://doi.org/10.1113/JP272613.
24. Sakata T. Pitfalls in short-chain fatty acid research: a methodological review. Anim Sci J. 2019;90:3–13. https://doi.org/10.1111/asj.13118.
25. Takagi T, et al. The influence of long-term use of proton pump inhibitors on the gut microbiota: an age-sex-matched case-control study. J Clin Biochem Nutr. 2018;62:100–5. https://doi.org/10.3164/jcbn.17-78.
26. Howell MD, et al. Iatrogenic gastric acid suppression and the risk of nosocomial *Clostridium difficile* infection. Arch Intern Med. 2010;170:784–90. https://doi.org/10.1001/archinternmed.2010.89.
27. Kwok CS, et al. Risk of *Clostridium difficile* infection with acid suppressing drugs and antibiotics: meta-analysis. Am J Gastroenterol. 2012;107:1011–9. https://doi.org/10.1038/ajg.2012.108.

28. Su T, Lai S, Lee A, He X, Chen S. Meta-analysis: proton pump inhibitors moderately increase the risk of small intestinal bacterial overgrowth. J Gastroenterol. 2018;53:27–36. https://doi.org/10.1007/s00535-017-1371-9.
29. Bolyen E, et al. Reproducible, interactive, scalable and extensible microbiome data science using QIIME 2. Nat Biotechnol. 2019;37:852–7. https://doi.org/10.1038/s41587-019-0209-9.
30. Callahan BJ, et al. DADA2: high-resolution sample inference from Illumina amplicon data. Nat Methods. 2016;13:581–3. https://doi.org/10.1038/nmeth.3869.
31. Quast C, et al. The SILVA ribosomal RNA gene database project: improved data processing and web-based tools. Nucleic Acids Res. 2013;41:D590–6. https://doi.org/10.1093/nar/gks1219.
32. Yilmaz P, et al. The SILVA and 'All-species Living Tree Project (LTP)' taxonomic frameworks. Nucleic Acids Res. 2014;42:D643–8. https://doi.org/10.1093/nar/gkt1209.
33. Koo TK, Li MY. A guideline of selecting and reporting intraclass correlation coefficients for reliability research. J Chiropr Med. 2016;15:155–63. https://doi.org/10.1016/j.jcm.2016.02.012.
34. Freedman D, Lane D. A nonstochastic interpretation of reported significance levels. J Bus Econ Stat. 1983;1:292–8. https://doi.org/10.1080/07350015.1983.10509354.
35. MacKinnon JG, White H. Some heteroskedasticity-consistent covariance matrix estimators with improved finite sample properties. J Econom. 1985;29:305–25. https://doi.org/10.1016/0304-4076(85)90158-7.
36. Benjamini Y, Hochberg Y. Controlling the false discovery rate: a practical and powerful approach to multiple testing. J R Stat Soc Ser B. 1995;57:289–300. https://doi.org/10.1111/j.2517-6161.1995.tb02031.x.

Figures

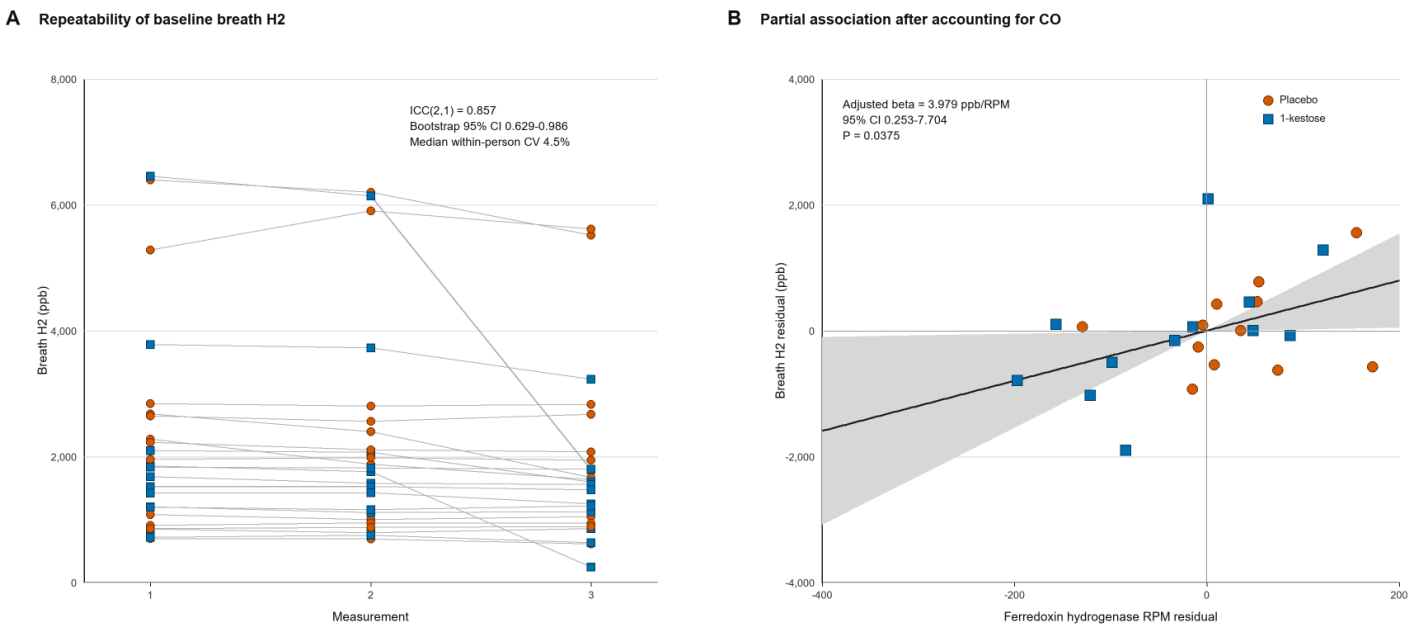


Figure 1

Repeatability of baseline breath H_2 measurements and their association with predicted Ferredoxin hydrogenase abundance.

(A) Three baseline breath H_2 measurements from each participant. Measurements from the same participant are connected by gray lines. Repeatability was quantified using a two-way-random, absolute-agreement, single-measure intraclass correlation coefficient (ICC[2,1]); its 95% CI was obtained by 20,000 participant-level bootstrap resamples. (B) Added-variable plot for the prespecified model median breath H_2 ~ Ferredoxin hydrogenase RPM + median breath CO. Median breath H_2 and Ferredoxin hydrogenase RPM were each residualized with respect to median breath CO for visualization. The solid line represents the partial regression coefficient, and the gray region is bounded by its two 95% confidence-limit slopes. Inferential statistics were obtained from the full OLS model rather than from a separately defined CO-corrected H_2 variable. Orange circles denote placebo and blue squares denote 1-kestose. n = 24.

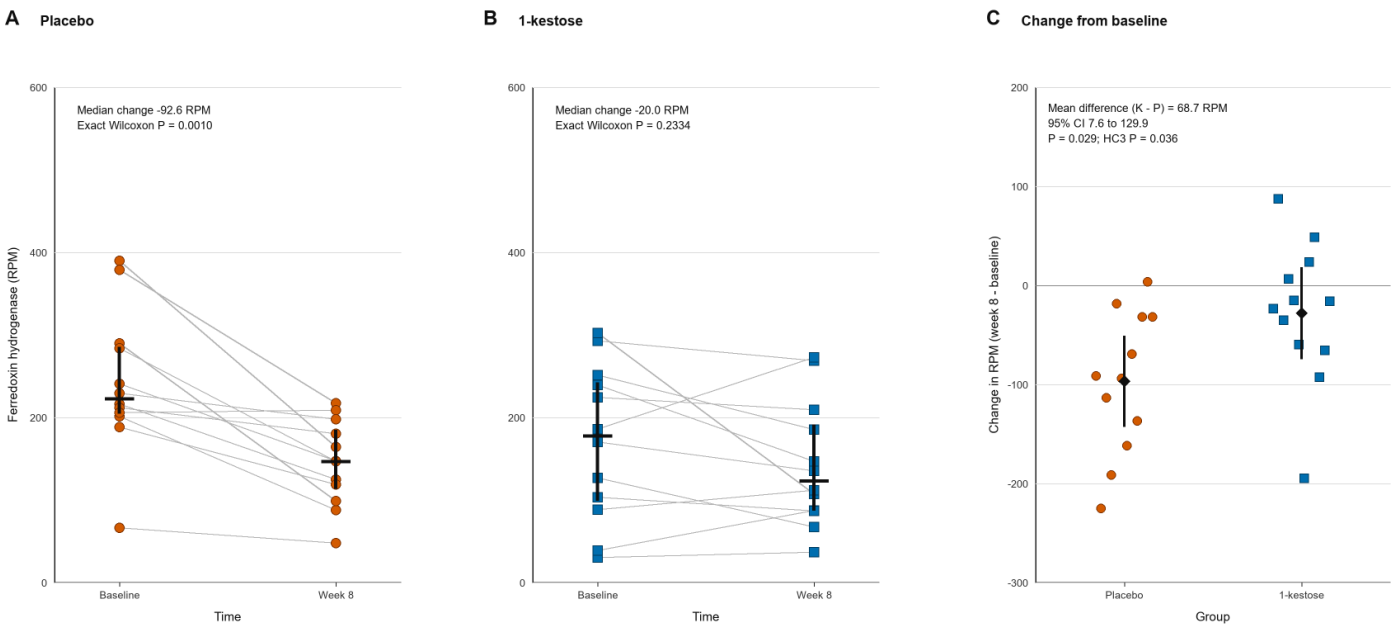


Figure 2

Longitudinal change in predicted Ferredoxin hydrogenase abundance.

(A, B) Paired baseline and week-8 abundances in the placebo (A) and 1-kestose (B) groups. Gray lines connect samples from the same participant. Horizontal black bars indicate medians, and vertical black bars indicate IQRs. Within-group P values were obtained from exact two-sided signed-rank randomization tests. (C) Participant-level changes calculated as week 8 minus baseline. Black diamonds and error bars indicate group means and 95% CIs. The between-group estimate is the mean change-score difference (1-kestose minus placebo) from OLS; the HC3 P value is shown as a robust sensitivity analysis. Orange circles denote placebo and blue squares denote 1-kestose. n = 12 per group.

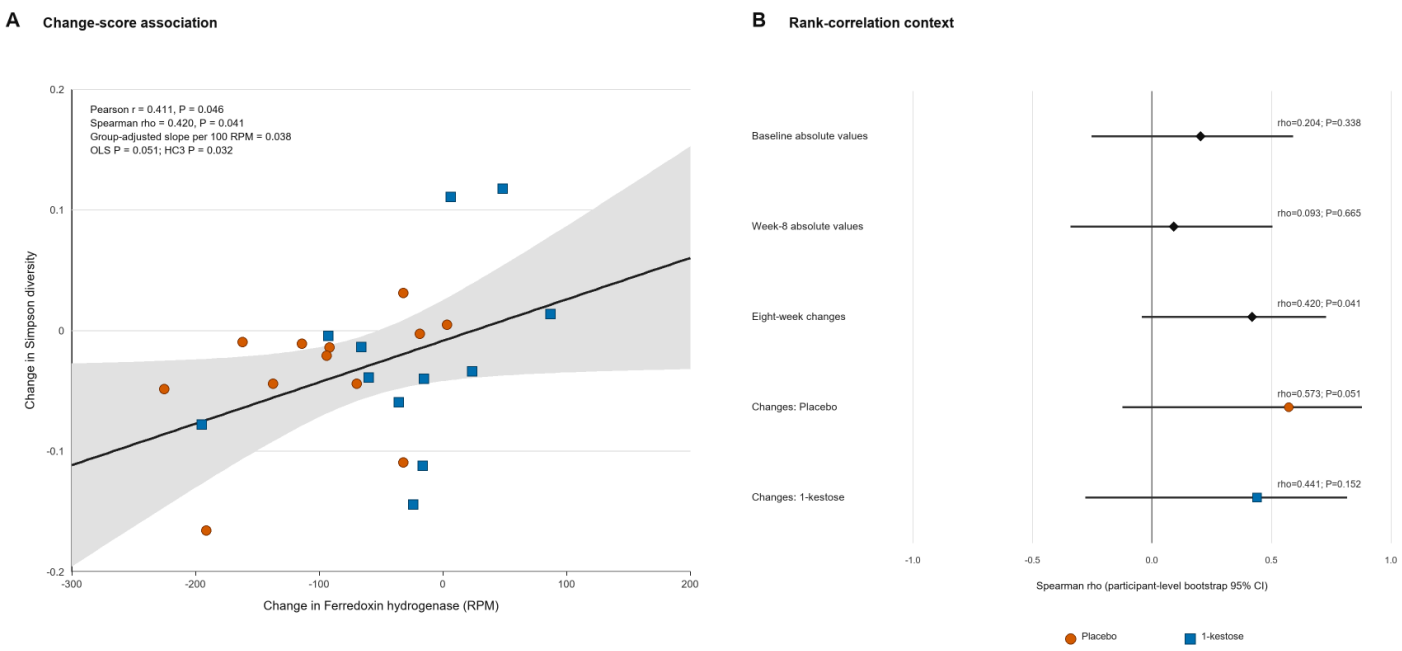


Figure 3

Association between eight-week changes in predicted Ferredoxin hydrogenase abundance and Simpson diversity.

(A) Participant-level changes calculated as week 8 minus baseline. The solid black line is the unadjusted OLS regression line, and the gray band indicates the 95% CI for the mean fitted response. The group-adjusted slope is reported per 100-RPM greater Ferredoxin change; conventional and HC3-robust P values are shown. (B) Spearman rank correlations for baseline absolute values, week-8 absolute values, overall eight-week changes, and group-specific eight-week changes. Symbols indicate correlation coefficients, and horizontal lines indicate participant-level percentile-bootstrap 95% CIs from 20,000 resamples. Orange circles denote placebo and blue squares denote 1-kestose; black diamonds denote estimates including both groups. Negative change values indicate a decline. n = 24 overall and n = 12 per group.

Supplementary Files

This is a list of supplementary files associated with this preprint. Click to download.

- SupplementaryTablesS1S7.xlsx
- SupplementaryTablesS1S7.xlsx
- SupplementaryFigureS1.tiff
- SupplementaryFigureS2.tiff
- SupplementaryFigureS3.tiff

- SupplementaryFigureS4.tiff
- SupplementaryFigureS5.tiff